Journal of ELECTRONIC MATERIALS, Vol. 42, No. 5, 2013
DOI: 10.1007/s11664-013-2558-3

Growth and Characterization of $In_xGa_{1-x}N$ Multiple Quantum Wells Without Phase Separation

P.V. WADEKAR,[1] Q.Y. CHEN,[1,2] H.C. HUANG,[3] Y.T. LIN,[1] C.W. CHANG,[1] H.W. SEO,[4] T.W. DUNG,[1] M.C. CHOU,[3] S.W. FENG,[5] N.J. HO,[3] D. WIJESUNDERA,[2] W.K. CHU,[2] and L.W. TU[1,6]

1.—Department of Physics and Center for Nanoscience and Nanotechnology, National Sun Yat-Sen University, Kaohsiung 80424, Taiwan, ROC. 2.—Department of Physics and Texas Center for Superconductivity, University of Houston, Houston, TX 77204, USA. 3.—Department of Materials and Opto-electronic Science, National Sun Yat-Sen University, Kaohsiung 80424, Taiwan, ROC. 4.—Department of Physics, University of Arkansas, Little Rock, AR 72204, USA. 5.—Department of Applied Physics, National University of Kaohsiung, Kaohsiung 81148, Taiwan, ROC. 6.—e-mail: lwtu@faculty.nsysu.edu.tw

Efficient conversion of photon energy into electricity is a crucial step toward a sustainable solar-energy economy. Likewise, solid-state lighting devices are gaining prominence because of benefits such as reduced energy consumption and reduced toxicity. Among the various semiconductors investigated, $In_xGa_{1-x}N$ alloys or superlattices are fervently pursued because of their large range of bandgaps between 0.65 eV and 3.4 eV. This paper reports on the fabrication of multiple quantum wells on $LiGaO_2$ (001) substrates by plasma-assisted molecular beam epitaxy. Metal modulated epitaxy was utilized to prevent formation of metal droplets during the growth. Streaky patterns, seen in reflection high-energy electron diffraction, indicate two-dimensional growth throughout the device. Postdeposition characterization using scanning electron microscopy also showed smooth surfaces, while high-resolution x-ray diffraction and high-resolution transmission electron microscopy confirm the epitaxial nature of the overall quantum well structure.

Key words: Group III nitride, MBE, solar cell, quantum well, InN, GaN, superlattice

INTRODUCTION

Group III nitrides have been studied for various optoelectronic devices such as light-emitting diodes (LEDs), photodetectors, and solar cells. Mixing of InN with GaN to form pseudobinary $In_{1-x}Ga_xN$ alloys allows one to tune the bandgap to match with various ranges of the solar spectrum.[1] In today's modern world, the demands for clean energy and proper energy usage with minimum wastage have made InGaN a viable candidate. So, InGaN-based photovoltaic solar cell devices provide a promising path to green energy technologies[2] as the efficiency of conversion continues to improve and the cost of fossil energy keeps rising. Moreover, III-nitride heterostructures can now be grown on Si wafers with proper buffers,[3] enabling integration of III-nitride solar cells with the better-developed traditional Si technology. Multijunction solar cells are considered to be more efficient than single-junction solar cells because, in theory, they could concurrently convert photon energies in various regions of the solar spectrum into electric current. Likewise, InGaN-based LEDs are also useful for green energy because of their low power consumption, long life, nontoxicity, and other attractive features. One of the key points is the effective tunability of the bandgap of group III nitrides that would be obtained if InN and GaN were to form homogeneous alloys without phase separation. Unfortunately, $In_xGa_{1-x}N$-based nitrides are notorious for their

(Received August 15, 2012; accepted March 1, 2013; published online April 9, 2013)

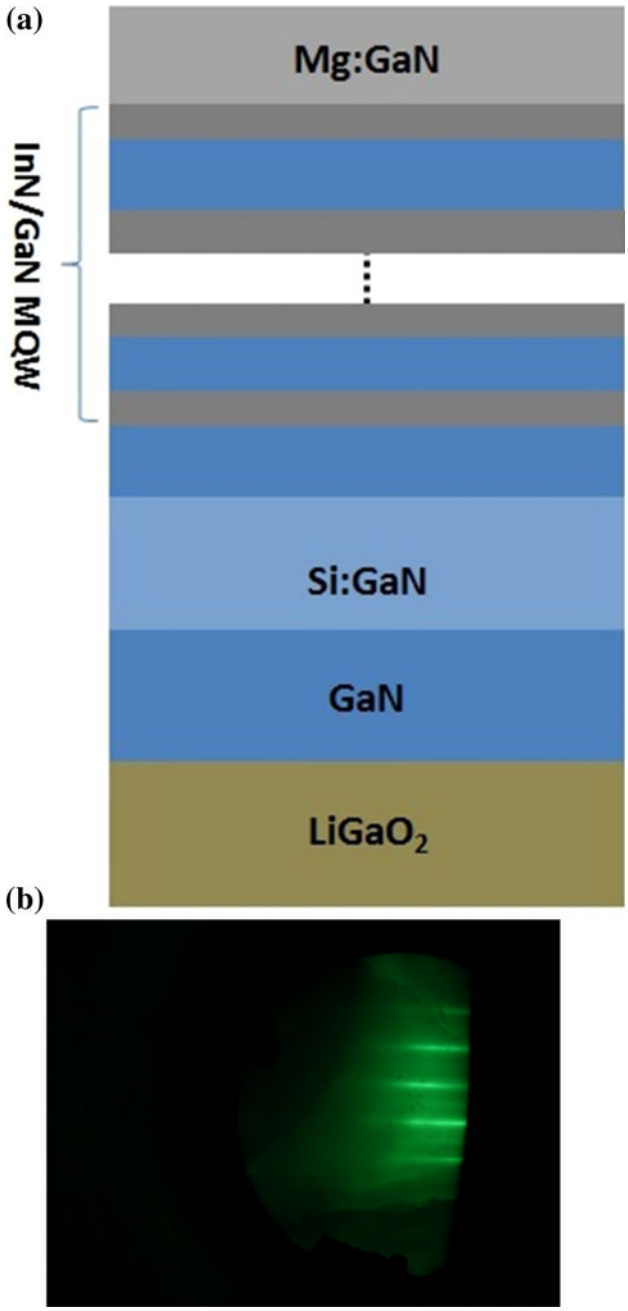

Fig. 1. (a) schematic of the *p*–i–*n* structure, and (b) RHEED image taken during the growth along GaN [10$\bar{1}$0] direction.

phase-separation problems in which the alloys dissociate into a mixture of indium-rich and indium-poor phases. This would certainly adversely affect device performance for either solar cells or LEDs. In this paper, we report on an effort to overcome such problems by growing ultrathin multiple quantum wells (MQWs) of GaN and InN at a temperature well above its dissociation temperature to foster high-quality epitaxial growth. We anticipate that such samples will not exhibit phase separation and that one could tune the bandgap by adjusting the thickness ratio of GaN to InN. The samples are characterized by high-resolution x-ray diffraction (HRXRD), high-resolution transmission electron microscopy (HRTEM), and cathodoluminescence (CL).

EXPERIMENTAL PROCEDURES

Orthorhombic $LiGaO_2$ (001) substrate provides an excellent lattice match to hexagonal GaN (0001).[4] The mismatch along the $[100]_{LGO}$ || $[1\bar{1}00]_{GaN}$ direction is 0.19%, while that along the $[010]_{LGO}$ || $[11\bar{2}0]_{GaN}$ direction is 1.9%. Such low lattice mismatch allows growth of highly epitaxial thin films. The heterostructure was grown on $LiGaO_2$ (001) substrates using plasma-assisted molecular beam epitaxy (PAMBE). By controlling the Ga, In, and N_2 fluxes, and the substrate temperatures, we could achieve thin films with very smooth interfaces—an important requirement for the growth of MQWs. The samples were grown in a Veeco EPI Gen930 MBE system equipped with nitrogen plasma as nitrogen source. Before the growth, substrates were ultrasonically cleaned in acetone and isopropyl alcohol (IPA) and loaded into the growth chamber. Reflection high-energy electron diffraction (RHEED) images were taken before deposition, and if the substrates did not show any pattern, indicative of lack of good surface, they were taken out to be annealed *ex situ* in a tube furnace at 1100°C for 8 h in flowing O_2 gas. This annealing step is critical for proper growth of the nitride thin films,[5] and proof of a RHEED pattern with clear diffraction spots is a criterion for selection of substrates. Also, the Ga and In fluxes were calibrated to 6.6×10^{-8} Torr by adjusting the effusion cell temperatures at which a base pressure of 5×10^{-9} Torr was maintained while all source shutters were closed. The N_2 flow rate was controlled by a mass flow controller to be fixed at 3×10^{-6} Torr when all other sources were closed. The V/III ratio during the growth of the whole structure was thus about 45. The typical growth temperatures for GaN using MBE are in the range between 670°C and 710°C, while those for InN are much lower, at 450°C to 550°C, beyond which InN becomes unstable. Thus, to grow GaN/InN superlattices, the substrate growth temperature is critical, as too high a growth temperature can lead to decomposition of InN, while too low a temperature can have a negative effect on the crystalline quality of GaN. Yoshikawa and coworkers have shown that a few monolayers of InN can be stable on GaN surface at high temperatures.[6] From their work, it is seen that InN monolayers can be inserted into a GaN matrix. Using this concept, combined with metal modulated epitaxy (MME),[7] we managed to grow a superlattice structure. MME involves periodic opening and closing of the metal fluxes, while the N_2 shutter is always kept open. Our growth window was slightly on the metal-rich side, so by using MME, if a Ga or In metal droplet is formed, the excess nitrogen will react with it to form nitride compound. GaN and Si:GaN were grown at 710°C;

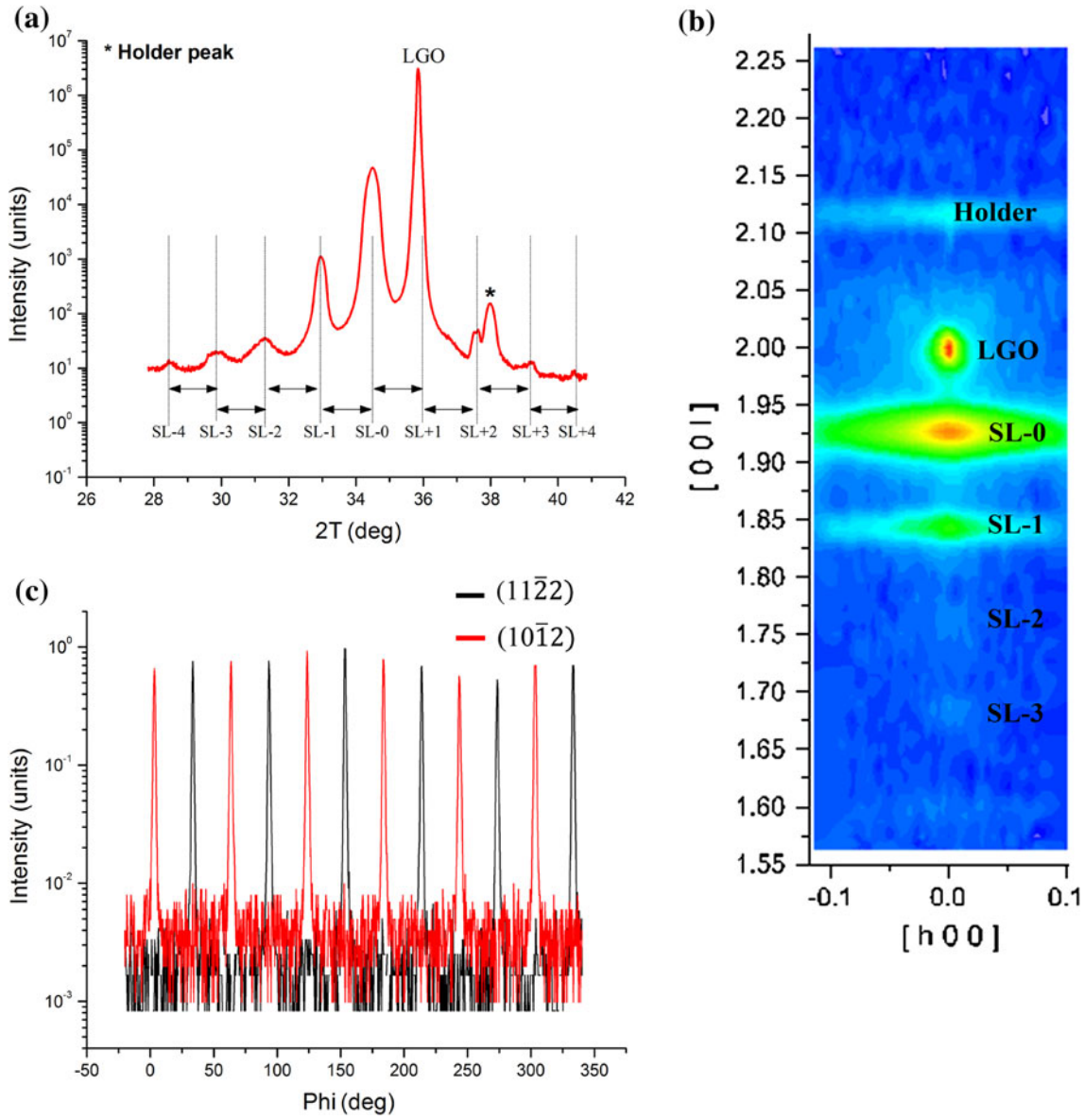

Fig. 2. (a) HRXRD pattern showing the satellite peaks, (b) symmetric RSM measurements, and (c) phi scans for the asymmetric film peaks.

InN/GaN MQWs and Mg:GaN were grown at 635°C. After the growth, the sample was quickly cooled to 500°C at a rate of 10°C/min to minimize any thermal effects on the InN layer and then slowly cooled to room temperature at a rate of 3°C/min from 500°C to room temperature to prevent the film from peeling off the substrate.

HRXRD was done on a Bede D1 high-resolution x-ray diffractometer, while an FEI transmission electron microscope was used for high-resolution atomic imaging and selected-area electron diffraction (SAED). A JEOL scanning electron microscope (SEM) with a Gatan detector was used to measure the temperature-dependent CL of these samples.

RESULTS AND DISCUSSION

Figure 1a shows a schematic of the *p*–i–*n* device, consisting of a stack of InGaN MQWs sandwiched by the Mg:GaN *p*-layer and Si:GaN *n*-layer. Figure 1b shows the RHEED pattern taken during the growth of the heterostructure. The streaky pattern indicates that the growth mode is Frank–van der Merwe or layer-by-layer in nature. Similar growth patterns were observed throughout the growth.

The films were further characterized by HRXRD, phi scans, and reciprocal-space mapping (RSM)

In Fig. 2a, the HRXRD diffraction pattern of the device is shown. The peak labeled “SL-0” is due to the bulk of the sample that conforms to the lattice constant of GaN. The satellite peaks up to the

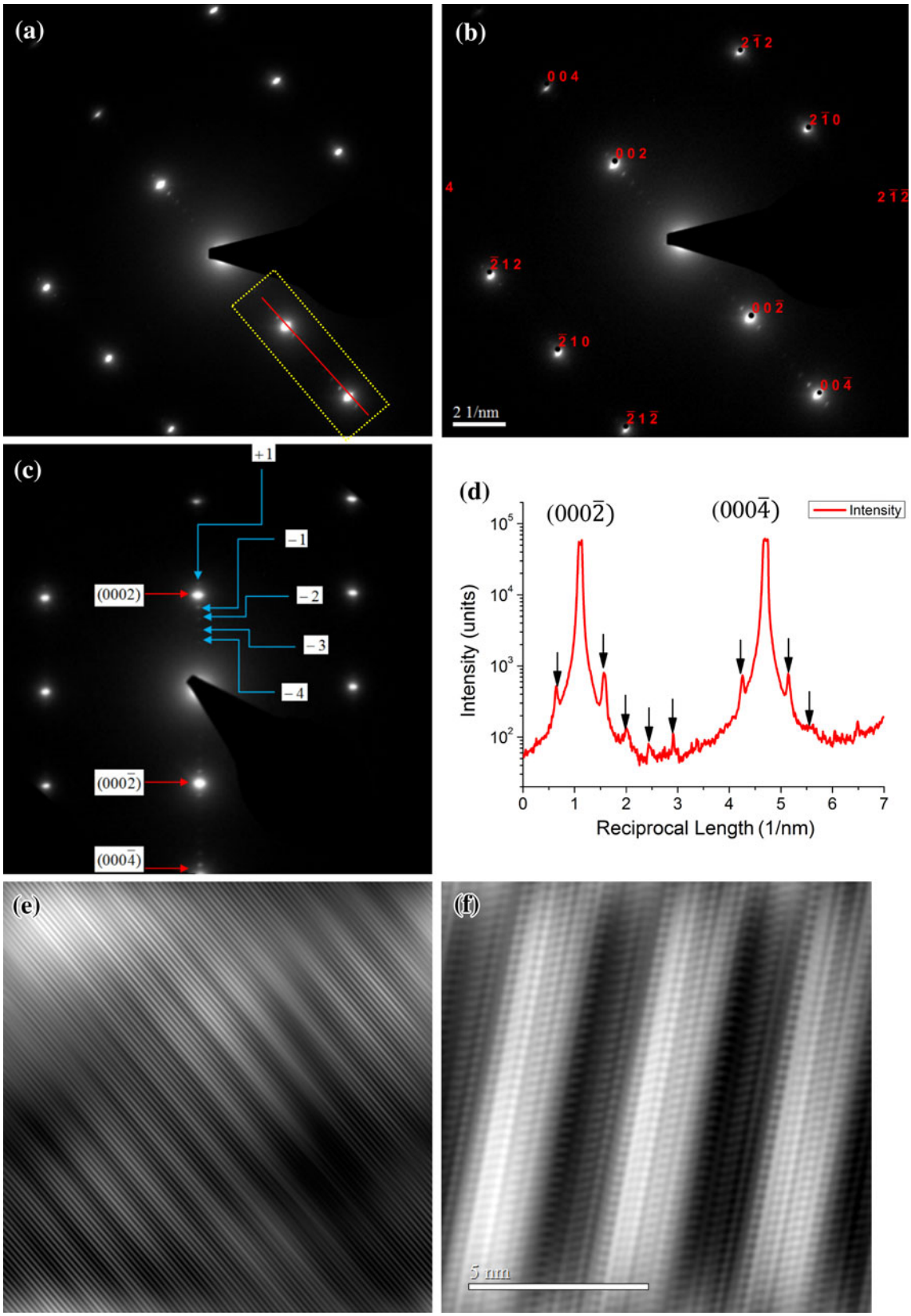

Fig. 3. (a) Exact zone SAED, (b) simulation of the diffraction pattern, (c) magnified image showing the satellite peaks, (d) line scan of the satellite peaks, (e) lattice fringe images, and (f) high-resolution atomic fringe images (Color figure online).

fourth order due to the MQW structure are also observed, labeled as "SL-n," with $n = -4, -3, -2, -1, +1, +2, +3$, and $+4$. No peaks due to InGaN or InN are observed, indicating that no mixed phases are formed. The full-width at half-maximum (FWHM) of the rocking curves for SL-0 and SL-1 are approximately 2000 arcseconds. The in-plane phi scans for the $(11\bar{2}2)$ plane, which shares the same zone axis as the a-plane $(11\bar{2}0)$ ($\omega = 34.5512°$, $2\theta = 69.1025°$, $\chi = -58.4067°$), shows a clear sixfold symmetry in the diffraction peaks. Similarly, the phi scans for the $(10\bar{1}2)$ plane, which shares the same zone-axis as the m-plane $(10\bar{1}0)$ ($\omega = 24.0489°$, $2\theta = 48.0979°$, $\chi = -43.1894°$), also shows a similar sixfold symmetry. These peaks are 30° displaced, as they should be for the planes of a- and m-zone axes. From the phi scans, therefore, one can infer that there is no intermixing of the m-plane and a-plane oriented phases. The rocking curve FWHMs for these asymmetric peaks are ~3000 arcseconds. Symmetric RSM measurements for the superlattice sample are shown in Fig. 2c. The SL-0 peak and the weaker satellite peaks are, much like their ω–2θ scan counterparts, all observed too. Overall, from the XRD data, one can conclude that the sample is epitaxial without any intermixing. We stress the intermixing issue because we intended to include more indium in the MQW layer of the heterostructure by growing at a lower temperature of 610°C. As a result of this, however, the XRD data show two other noticeable changes. First, the FWHM of the rocking curves become broader, indicating that the overall film quality degrades at lower growth temperatures. Secondly, intermixing between the m- and a-plane starts to emerge as judged by the asymmetry in the phi-scan curves. This indicates that reducing the growth temperature damages the epitaxial quality. Conversely, increasing the growth temperature to 710°C resulted in pure GaN film—no satellite peaks or superlattice peaks were seen. At such a high temperature, only GaN film is stable. Thus, the growth window for the InN/GaN MQW is very narrow, from ~635°C to 650°C. The substrate temperature for our system is measured using two methods. The first one is a thermocouple below the substrate, while the second one is an optical pyrometer. In the substrate transfer mode, the substrate heater faces an optical viewport. We use this optical viewport to measure the temperature of the sample surface using an optical pyrometer. The temperature measured by the optical pyrometer is 10°C to 12°C lower than the one measured by the thermocouple.

HRTEM measurements were conducted to further study the structure of the samples grown at 635°C. For TEM measurement, the samples were cut in two orthogonal cross sections parallel to the $[100]_{LGO}$ and $[010]_{LGO}$ directions. In the figures below, we show representative measurements for one such set of samples.

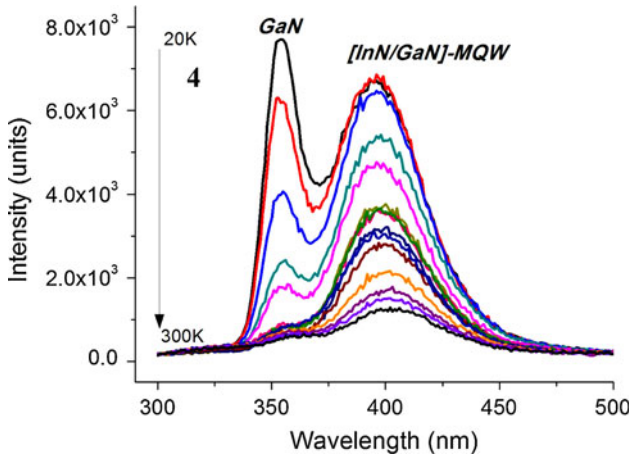

Fig. 4. Temperature-dependent cathodoluminescence for the heterostructure.

Figure 3a shows the exact zone SAED pattern for the MQW region of the p–i–n structure. One can see the main diffraction peaks accompanied by some smaller satellite peaks. In Fig. 3b, the diffraction pattern and its simulation are shown. This simulation was done using SingleCrystal software, indicating that the zone axis is $[11\bar{2}0]$. The parameters used for the simulation were those of bulk GaN, namely lattice constants $a = 3.189$ Å, $c = 5.185$ Å and angles $\alpha = 90°$, $\beta = 90°$, $\gamma = 120°$. As seen, the simulation fits well with the SAED data. The magnified SAED pattern highlighted by the rectangular box in Fig. 3a shows the diffraction spots, as given in Fig. 3c, containing the main peaks as well as the weaker satellites up to the fourth order, much like the XRD results discussed above, corresponding to the peaks of SL-0 from the GaN film and SL-4, SL-3,…,SL+4 due to the superlattice structure. Shown in Fig. 3d, a line scan (red line in Fig. 3a) bears this out. In Fig. 3e, we show lattice fringe images of the MQW region. The lattice image shows clear contrast of smooth interfaces between periodically alternating GaN and InN layers. A higher-magnification atomic image detailing the quantum well structure is shown in Fig. 3f. The white regions represent the GaN layers, while the black regions represent the InN layers. Some small intermixing is seen between the two layers, which could result from the formation of some $In_{1-x}Ga_xN$. In spite of this, the interfaces are by and large smooth at the atomic scale. In brief, from the SAED diffraction pattern, as verified by the simulations, the bulk of two p- and n-doped GaN layers are largely relaxed while the InN layers are coherently strained to the neighboring GaN layers in the superlattice with consistent periodicity and smooth interface.

The optical properties of these samples were studied by CL measurements. Figure 4 shows the temperature-dependent measurements. A sharper peak near 350 nm due to the GaN is observed,

accompanied by a broad peak due to the InN/GaN MQWs at 400 nm. From the peak position, the indium percentage is evaluated to be about 10%. Time-resolved photoluminescence indicates a room-temperature carrier lifetime of 1.4 ns. For samples where the MQWs were grown at lower temperature of 610°C, a similar CL spectrum was observed but the carrier lifetime could not be measured. This could possibly be due to the fact that defects caused by intermixing lead to nonradiative recombination of electron–hole pairs.

CONCLUSIONS

We have shown that it is possible to grow coherently strained MQWs of InN/GaN as the intrinsic layer in a *p*–i–*n* heterostructure. The indium doping level is ~10%. No phase separation or spinodal decomposition-related phenomena were observed in the samples. HRTEM images and SAED diffraction patterns confirm the formation of the quantum well structure as seen from the atomic imaging and satellite peaks, respectively. Our work shows that quantum well-based structures are experimentally possible and can be a useful strategy for optoelectronic devices. The MQW growth temperature is an important factor, since it will change the sample structure. This, in turn, could change the carrier lifetime and thus affect the device performance. Further optimization of the growth process and improvement in the crystal quality could result in the design of a device structure wherein one can tune the bandgap to the desired level by adjusting the quantum well structure or grow nested superlattices. An improvement in the quality by further optimization of the growth process will also help in increasing the carrier lifetime of the samples, thus improving the device performance.

ACKNOWLEDGEMENTS

This work was supported in part by the National Science Council, Taiwan, Republic of China, under Grant NSC 101-3113-E-110; facilities at the Center for Nanoscience and Nanotechnology were used. Work at UH and UALR is supported in part by the National Science Foundation under Grant No. DMR-0404542, EPS-1003970, in part by the Department of Energy through Grant No. DE-FG02-05ER46208, in part by the US Air Force Office of Scientific Research through Grant No. FA9550-06-1-0401, and in part by the State of Texas Strategic Partnership for Research in Nanotechnology (SPRING) through the Texas Center for Superconductivity at the University of Houston.

REFERENCES

1. J. Wu, W. Walukiewicz, K.M. Yu, W. Shan, J.W. Ager, E.E. Haller, H. Lu, W.J. Schaff, W.K. Metzger, and S. Kurtz, *J. Appl. Phys.* 94, 6477 (2003).
2. R.H. Bube, *Photovoltaic Materials* (London: Imperial College Press, 1988).
3. L.A. Reichertz, I. Gherasoiu, K.M. Yu, V.M. Kao, W. Walukiewicz, and J.W. Ager III, *Appl. Phys. Express*. 2, 122202 (2009).
4. R.J. Matyi, W.A. Doolittle, and A.S. Brown, *J. Phys. D: Appl. Phys.* 32, A61 (1999).
5. G. Lia, S. Muc, and S.J. Shihb, *Mater. Sci. Eng. B.* 170, 14 (2010).
6. A. Yoshikawa, S.B. Che, W. Yamaguchi, H. Saito, X.Q. Wang, Y. Ishitani, and E.S. Hwang, *Appl. Phys. Lett.* 90, 073101 (2007).
7. M. Moseley, D. Billingsley, W. Henderson, E. Trybus, and W.A. Dolittle, *J. Appl. Phys.* 106, 014095 (2009).